Journal of Power Sources 354 (2017) 207–214

Contents lists available at ScienceDirect

Journal of Power Sources

journal homepage: www.elsevier.com/locate/jpowsour

Thermal conductivity of catalyst layer of polymer electrolyte membrane fuel cells: Part 1 — Experimental study

Mohammad Ahadi [a], Mickey Tam [b], Madhu S. Saha [b], Jürgen Stumper [b], Majid Bahrami [a, *]

[a] Laboratory for Alternative Energy Conversion (LAEC), School of Mechatronic Systems Engineering, Simon Fraser University, Surrey, BC, V3T 0A3, Canada
[b] Automotive Fuel Cell Cooperation, 9000 Glenlyon Parkway, Burnaby, BC, V5J 5J8, Canada

HIGHLIGHTS

- A new method is proposed for measuring thermal conductivity of catalyst layers.
- An accurate method is proposed for measuring thickness of catalyst layers.
- Effects of contact and residual resistances are deconvoluted from the data.
- Effects of hot-pressing, compression, testbed, and substrate are studied.
- The obtained thermal conductivity data are compared to an analytical model.

ARTICLE INFO

Article history:
Received 25 November 2016
Received in revised form
4 February 2017
Accepted 6 February 2017
Available online 24 February 2017

Keywords:
Polymer electrolyte membrane fuel cell
Catalyst layer
Through-plane thermal conductivity
Thermal contact resistance
Transient plane source
Guarded heat flow

ABSTRACT

In this work, a new methodology is proposed for measuring the through-plane thermal conductivity of catalyst layers (CLs) in polymer electrolyte membrane fuel cells. The proposed methodology is based on deconvolution of bulk thermal conductivity of a CL from measurements of two thicknesses of the CL, where the CLs are sandwiched in a stack made of two catalyst-coated substrates. Effects of hot-pressing, compression, measurement method, and substrate on the through-plane thermal conductivity of the CL are studied. For this purpose, different thicknesses of catalyst are coated on ethylene tetrafluoroethylene (ETFE) and aluminum (Al) substrates by a conventional Mayer bar coater and measured by scanning electron microscopy (SEM). The through-plane thermal conductivity of the CLs is measured by the well-known guarded heat flow (GHF) method as well as a recently developed transient plane source (TPS) method for thin films which modifies the original TPS thin film method. Measurements show that none of the studied factors has any effect on the through-plane thermal conductivity of the CL. GHF measurements of a non-hot-pressed CL on Al yield thermal conductivity of 0.214 ± 0.005 $W \cdot m^{-1} \cdot K^{-1}$, and TPS measurements of a hot-pressed CL on ETFE yield thermal conductivity of 0.218 ± 0.005 $W \cdot m^{-1} \cdot K^{-1}$.

1. Introduction

Polymer electrolyte membrane fuel cells (PEMFCs) are considered one of the future sources of clean energy due to their promising features, such as potentially zero greenhouse gas emissions, high efficiency, and abundance of their fuel source, i.e. hydrogen. Efficient operation of a typical automotive PEMFC occurs in a certain range of temperature from 60 °C to 80 °C [1]. At temperatures below 60 °C, the kinetics of the electrochemical reaction slows down, and the electrodes are prone to flooding as a result of product water saturation [2]. At temperatures above 80 °C, the membrane dries out, and consequently, ohmic losses attributed to proton transport through the membrane increase [2]. In addition to these performance consequences, PEMFCs face durability issues if they operate outside the mentioned temperature range; breaking down of the membrane at high temperatures due to its glass transition at temperatures around 80 °C as well as damage to various components of the fuel cell due to ice expansion during freezing are some of the reported durability issues [1]. Accordingly, water management, thermal management, and degradation minimization are highly and intricately correlated to each other, among

* Corresponding author.
E-mail addresses: mahadi@sfu.ca (M. Ahadi), Mickey.Tam@afcc-auto.com (M. Tam), Madhu.Saha@afcc-auto.com (M.S. Saha), Juergen.Stumper@afcc-auto.com (J. Stumper), mbahrami@sfu.ca (M. Bahrami).

http://dx.doi.org/10.1016/j.jpowsour.2017.02.016
0378-7753/

Nomenclature

A	Cross sectional area of the testbed sensor(s) (m^2)
k	Thermal conductivity ($W \cdot m^{-1} \cdot K^{-1}$)
R	Thermal resistance ($K \cdot W^{-1}$)
R'	A share of the bulk resistance of the substrate-CL-CL-substrate sandwich excluding the bulk resistance of the catalyst layer ($K \cdot W^{-1}$), $R' = 2R_{b,sub} + 2R_{c,sub-cl} + R_{c,cl-cl}$
P	Mechanical pressure (Pa)
R''	A constant resistance ($K \cdot W^{-1}$), $R'' = R' + R_{res}$
t	Thickness (m)

Subscripts

b	Bulk property
c	Contact
cl	Catalyst layer
res	Residual
s	Sample
san	Sandwich
sub	Substrate
tot	Total

which thermal management can be considered as the core controlling factor which directly affects the others. Effective thermal management is hinged on having detailed knowledge about temperature distribution inside various layers of the membrane electrode assembly (MEA), and the key to finding such information is an in-depth knowledge of thermal conductivity of different components of the MEA.

So far, some studies have been performed on thermal conductivity of different MEA components [3–25]. However, the reported studies on the thermal conductivity of catalyst layers (CLs) [3,16,17,25] are purely experimental, and the reported data in literature contain effects of thermal contact resistances (TCRs) together with some other residual bulk resistances present in the measurements, whose effects are uncertain and not debated much in literature. Khandelwal and Mench [3] measured the effective through-plane thermal conductivity of various fuel cell materials using the guarded heat flow (GHF) method [26] and reported 0.27 ± 0.05 ($W \cdot m^{-1} \cdot K^{-1}$) for the through-plane thermal conductivity of some CLs, deconvoluted from measurements of an MEA. As mentioned in Ref. [3], this is an effective thermal conductivity that also contains the TCRs between the CLs and the gas diffusion layers (GDLs) as well as the TCRs between the CLs and the membrane. Alhazmi et al. [16] employed the parallel thermal conductance (PTC) technique [27] and measured the in-plane thermal conductivity of some CLs by deconvoluting the thermal conductivity from measurements of an MEA and catalyst-coated GDLs, neglecting: 1) the TCRs between the GDLs and the CLs present in measurements of both the MEA and the catalyst-coated GDLs, 2) the TCRs between the membrane and the CLs in the MEA, and 3) possible effects of compression of the MEA on thermal conductivity of the MEA components. Alhazmi et al. [16] reported insensitivity of the in-plane thermal conductivity to temperature, its slight increase with Pt loading (in terms of mg_{Pt}/cm^2), and in-plane thermal conductivity values of 0.29–0.39 $W \cdot m^{-1} \cdot K^{-1}$. Alhazmi et al. [17] used a GHF device to measure the through-plane thermal conductivity of catalyst-coated GDLs (spray-coated) and deconvoluted the through-plane thermal conductivity of the CLs from measurements of the catalyst-coated GDLs, neglecting TCRs present in their measurements including the TCRs between the CLs and the GDLs. Alhazmi et al. [17] reported insensitivity of the through-plane thermal conductivity to temperature and ~0.34 $W \cdot m^{-1} \cdot K^{-1}$ for through-plane thermal conductivity of a 0.4 mg_{Pt}/cm^2 CL which was comparable with the in-plane thermal conductivity of the same CL. Burheim et al. [25] made CLs (~30 and 60 μm thick) by spraying several layers of the catalyst ink onto copper substrates, stacked copper-catalyst-aluminum sandwiches in a GHF device, and reported overall through-plane thermal conductivity values of 63–98 $mW \cdot m^{-1} \cdot K^{-1}$ for dry CLs with different compositions under compression; they neglected the effects of thermal resistances of the metal foils and TCRs within the stacks.

In the first part of this study, a new methodology, which eliminates the effects of any possible TCR in the through-plane measurements by the GHF method [26] or the modified transient plane source (TPS) method for thin films [19], is introduced for measurement of through-plane thermal conductivity of CLs. The new methodology is also employed to investigate effects of hot-pressing/decal-transfer, compression, measurement method, and substrate on through-plane thermal conductivity of some CLs. In the second part of this work [28], a novel analytical model is presented to predict the bulk thermal conductivity of a CL as a function of its salient geometrical parameters and operating conditions.

2. Experimental procedure

2.1. Sample preparation

For this study, several CLs with ionomer to carbon (I/C) weight (wt) ratio of 1.1 and 50 wt% Pt in Pt/C catalyst (carbon-supported platinum) were coated on ethylene tetrafluoroethylene (ETFE) and aluminum (Al) substrates. For this purpose, a dispersion of the catalyst ink containing catalyst powder, ionomer, and n-propanol was coated onto one side of ETFE sheets (100 μm thick) and Al foils (50 μm thick) by a Mayer bar coater, shown in Fig. 1. Four different Pt loadings of 0.24 and 0.50 mg/cm^2 on ETFE, corresponding to different thicknesses of 7 μm and 14 μm, and 0.13 and 0.34 mg/cm^2 on Al, corresponding to different thicknesses of 4 μm and 12 μm, were made using coating rods with different grades. The catalyst-coated substrates were then kept on a heated surface (50 °C) to dry out and were further left in the open to ensure the complete evaporation of all the volatile solvent. It is worthy to mention that in the present study, partially graphitized carbon was used. This point becomes important when considering that graphitization of carbon could increase the effective thermal conductivity of the carbon powder by a factor of almost six [29].

In the conventional method of MEA fabrication, a CL undergoes hot-pressing two times: once when the CL is decal-transferred from a substrate onto a membrane, and a second time, during the assembly of the MEA. For this reason, to study the possible effects of hot-pressing on thickness and thermal conductivity of the CL, some of the catalyst-coated substrates underwent the same hot-pressing conditions. The hot-pressing conditions were simulated by putting the samples under 150 °C temperature and 15 bar pressure for 3 min.

2.2. Thickness measurements

To examine the behavior of the CLs under compression, thicknesses of the catalyst-coated substrates were monitored under pressures from 1 to 30 bar with accuracy of 1 μm by using a custom-made testbed known by the name TUC_RUC at the industrial partner of the project, Automotive Fuel Cell Cooperation Corp. (AFCC). To make the effective thickness of a CL larger in the TUC_RUC device, two pristine pieces of the catalyst-coated substrate were made into a sandwich by contacting them from their

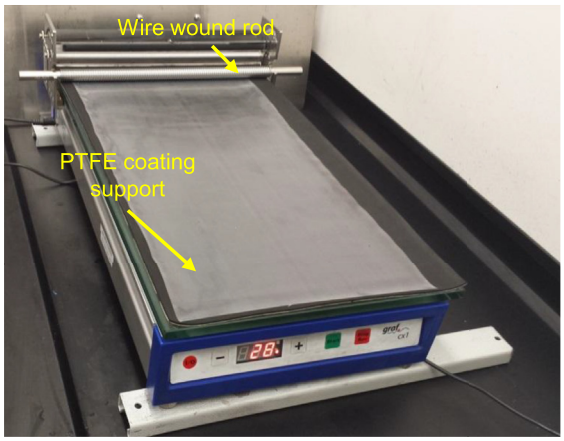

(a)

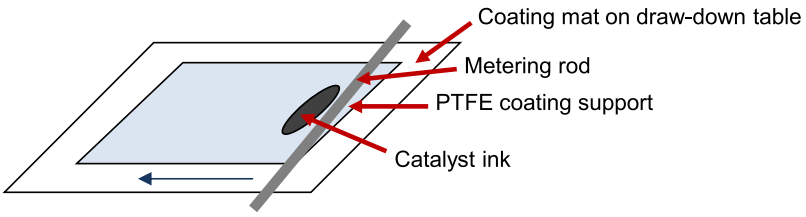

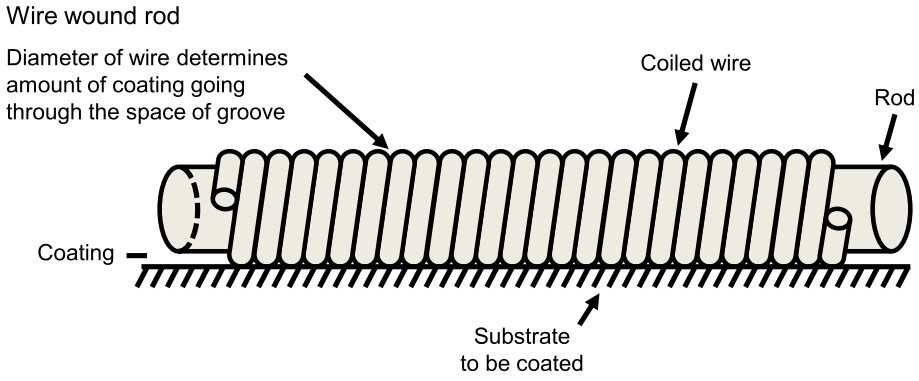

(b)

Fig. 1. Mayer bar coater: (a) a picture of the used Mayer bar, and (b) a schematic of the Mayer bar.

catalyst sides, and the sandwich was then put in between the mechanical jaws of the TUC_RUC device for thickness measurements. Moreover, to detect any possible change in the CL thickness due to hot-pressing/decal-transfer conditions, the same experiments were performed by the TUC_RUC device for hot-pressed catalyst-coated substrates; in addition, thickness of a pristine CL coated on ETFE substrate was measured by scanning electron microscopy (SEM) and compared to the thickness of the same CL after being decal-transferred by hot-pressing from a catalyst-coated ETFE sheet onto an NRE-211 membrane. For this purpose, an epoxy puck containing the mentioned sample was made by casting epoxy onto the sample; after curing the epoxy, the epoxy puck was polished from the sample cross section side by a lapping machine and, then, carbon-coated by a sputtering device. The thickness of the sample cross section was then measured by an SEM machine.

For thermal conductivity measurements, thickness of the CLs was measured by SEM on freeze-fractured samples in liquid nitrogen to ensure high quality cross section cuts and accurate thickness measurements. Due to the difficulty in freeze-fracturing ETFE samples, catalyst coated membranes (CCMs) were made instead by decal-transferring the CLs from ETFE onto NRE-211 membranes; then, the prepared CCMs were cut under liquid nitrogen by a sharp knife. On the other hand, the CLs coated on Al foil were not transferrable onto membrane by hot-pressing, and the catalyst-coated Al foils could not be cut sharply by the knife. Therefore, the catalyst-coated Al foils were directly cut under liquid nitrogen by sharp scissors. The cut samples, held vertically in an SEM sample holder shown in Fig. 2, were then dried at 80 °C in a vacuum oven for about an hour immediately after the freeze-

fracture step in order to avoid the absorption of ambient air humidity by the cold samples. Thickness of a CL was then measured by an SEM device at different locations along its cross section, and the average of the measured thicknesses along the cross section was used in further calculations. Fig. 3 shows SEM images of the samples along with the measured average thicknesses and standard deviations of thicknesses from the average values, clearly indicating the high uniformity of the prepared CLs in terms of thickness. Accuracy of the thickness measurements was better than 0.3 μm for CL transferred onto membrane and better than 0.06 μm for CL on Al, based on the pixel sizes and magnification of the taken SEM images.

2.3. Through-plane thermal resistance/conductivity measurements

Two methods are used in this study for measurements of through-plane thermal resistance: 1) steady state method by using a custom-made GHF device, as per ASTM Standard E1530-11 [26], and 2) transient method by using a modified transient plane source (TPS) method for thin films on a hot disk TPS2500S Thermal Constants Analyser (Hot Disk AB, Gothenburg, Sweden and ThermTest Inc., Fredericton, Canada) [19]. Schematics of the configuration of the samples in the GHF and TPS testbeds are shown in Fig. 4. The details of the methods and the relevant devices can be found elsewhere, see for example [9,19,26].

By placing a sample in the test column of a GHF device or a TPS testbed, a total through-plane resistance is measured for the sample which contains the through-plane bulk resistance of the sample and a residual part. In the case of the GHF device, the residual resistance consists of TCRs between the sample and the GHF fluxmeters [9,19,26], whereas in the case of the TPS testbed, the residual contains the effects of through-plane bulk resistance of the TPS sensor insulating layer and the TCRs in the TPS test column [19]. Therefore, the total through-plane resistance measured by either of the GHF or TPS devices can be written as follows:

$$R_{tot} = R_{b,s} + R_{res} \tag{1}$$

where $R_{b,s} = \frac{t_s}{k_s A}$ is the through-plane bulk resistance of the sample; t_s is the sample thickness; A is the cross sectional area of the testbed sensor(s), and R_{res} is the residual.

According to Eq. (1), there are two unknowns (k_s and R_{res}) for measurement of one thickness of a particular sample. Therefore, measurements of at least two thicknesses of the same sample, ideally with identical microstructure and surface features, are required to deconvolute the through-plane bulk thermal conductivity of the sample (k_s) from the raw experimental data. After doing measurements for two thicknesses of the same sample (t_1 and t_2), the through-plane bulk thermal conductivity of the sample can be deconvoluted from the measured total resistances ($R_{tot,1}$ and $R_{tot,2}$) by the following equation:

$$k_s = \frac{t_2 - t_1}{(R_{tot,2} - R_{tot,1})A} \tag{2}$$

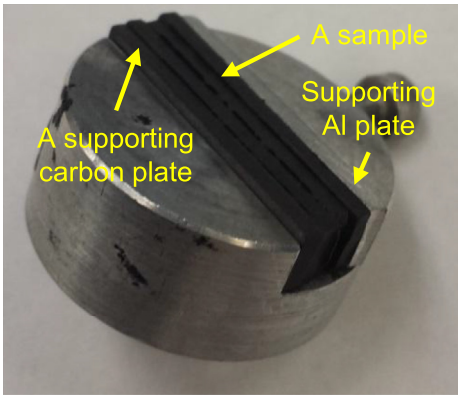

Fig. 2. The sample holder used for SEM imaging.

2.4. Sample configuration

CLs have a highly fragile microstructure and a very thin thickness (~4 μm), which makes having a stand-alone CL for the measurements impossible. For this reason, the measurements should be performed on catalyst-coated substrates, and the thermal conductivity of the CL could be determined from the results of such measurements. Accordingly, in this study, to maintain a reasonable amount of catalyst in the test column and, also, to avoid any contact between the fragile catalyst and the hard surfaces of the TPS thin film sensor or the GHF fluxmeters, two catalyst-coated substrates were made into a sandwich by contacting them from their catalyst sides. The resulting sandwich was considered as one sample for the measurements. A schematic of the mentioned configuration and the relevant thermal resistance network of the sandwich are shown in Fig. 5. It should be noted that, compared to a hypothetical stand-alone CL, the only differences resulted from stacking two substrate-CL samples in the test column are the addition of some constant resistances and doubling the bulk resistance of the CL. According to Fig. 5 b, the through-plane bulk resistance of a sandwich can be described by the following:

$$\begin{aligned} R_{b,san} &= R_{b,sub} + R_{c,sub-cl} + R_{b,cl} + R_{c,cl-cl} + R_{b,cl} + R_{c,sub-cl} + R_{b,sub} \\ &= 2R_{b,cl} + \left[2R_{b,sub} + 2R_{c,sub-cl} + R_{c,cl-cl}\right] \\ &= \frac{2t_{cl}}{k_{cl}A} + R' \end{aligned} \tag{3}$$

where $R' = 2R_{b,sub} + 2R_{c,sub-cl} + R_{c,cl-cl}$ is a share of the sandwich resistance which does not include the through-plane bulk resistance of the CL. As is clear from Eq. (3), when just the thicknesses of the CLs are changed in the sandwich, except for the through-plane bulk resistances of the CLs, the rest of the resistances remain constant, resulting in the resistances of two different sandwiches being just different in a constant, i.e. R'. By combining Eqs. (1) and (3), the measured total resistance of a substrate-CL-CL-substrate sandwich is expressed by:

$$R_{tot,san} = R_{b,san} + R_{res} = \frac{2t_{cl}}{k_{cl}A} + R' + R_{res} = \frac{t_{cl,tot}}{k_{cl}A} + R'' \tag{4}$$

where $R'' = R' + R_{res}$ is a constant and $t_{cl,tot} = 2t_{cl}$ is the total thickness of catalyst in the sandwich. Accordingly, the total through-plane resistance of a sandwich measured by either the modified TPS method or the GHF method is a linear function of the total thickness of the catalyst in the sandwich. Therefore, after performing measurements for two thicknesses of the catalyst in the sandwich, the through-plane bulk thermal conductivity of the catalyst can be deconvoluted by Eq. (2).

2.5. Uncertainty analysis

The uncertainty analysis of the steady state and transient methods is thoroughly described in Ref. [19] and is not repeated here for conciseness.

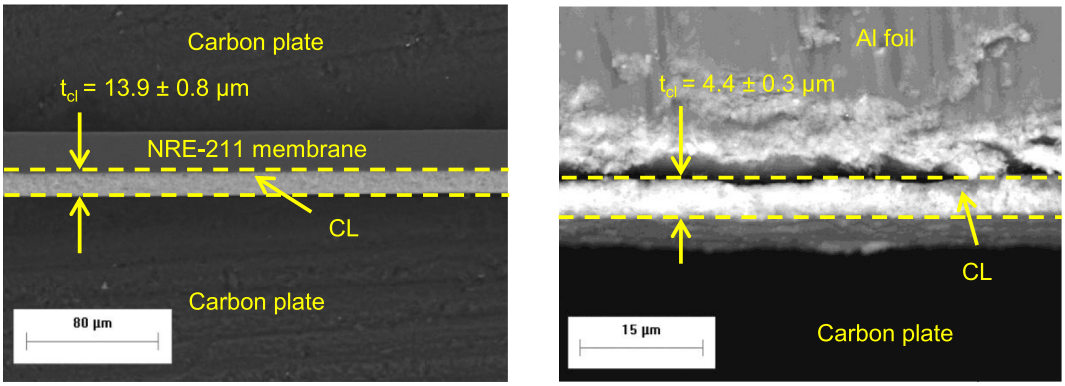

Fig. 3. SEM images of CL samples: (a) decal-transferred from ETFE onto membrane, and (b) coated on Al foil.

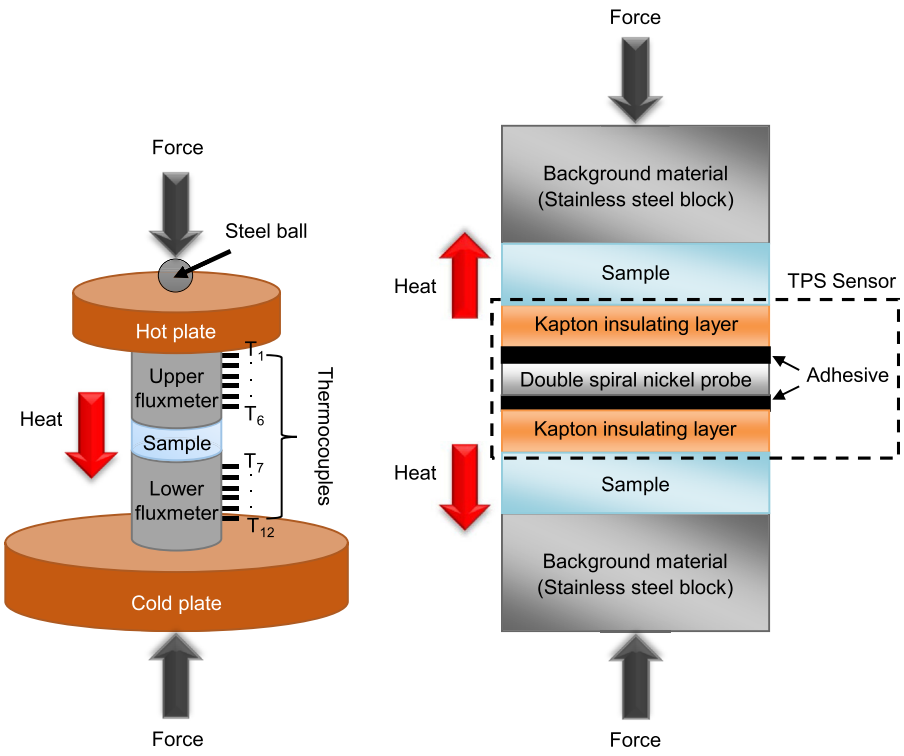

Fig. 4. Schematics of the configuration of the samples in the: (a) GHF testbed, and (b) TPS testbed.

3. Results and discussion

The results from the TPS testbed are plotted next to the results from the GHF testbed for the purpose of comparison, throughout this section. Since the area of the TPS sensor is different than the area of the fluxmeters of the GHF testbed, the measured values of thermal resistance per unit area, i.e. thermal insulance [$K \cdot mm^2 \cdot W^{-1}$], are compared.

The total through-plane thermal insulance versus pressure for different overall thicknesses of catalyst in the sandwich are shown in Fig. 6. As shown in Fig. 6, for each thickness of catalyst in a sandwich, the total insulance decreases with pressure due to reduction in the TCRs of the test columns with increasing pressure. In addition, the total insulance values measured by the modified TPS method are generally higher than the values measured by the GHF method due to: i) much higher resistance of the 100 µm thick ETFE substrates (having thermal conductivity of ~0.17 $W \cdot m^{-1} \cdot K^{-1}$ [19]) used for the modified TPS measurements compared to the 50 µm thick Al substrates (having thermal conductivity of ~205 $W \cdot m^{-1} \cdot K^{-1}$) used for the GHF measurements, and ii) extra bulk resistance of the Kapton layer in the TPS test column compared to the GHF test column [19]. The calculated maximum uncertainty for $R_{tot,san}A$ is 0.4% for the modified TPS method and 4.6% for the GHF method.

Change in $R''A$ versus pressure is plotted in Fig. 7 for the modified TPS and GHF measurements. As expected, the observed

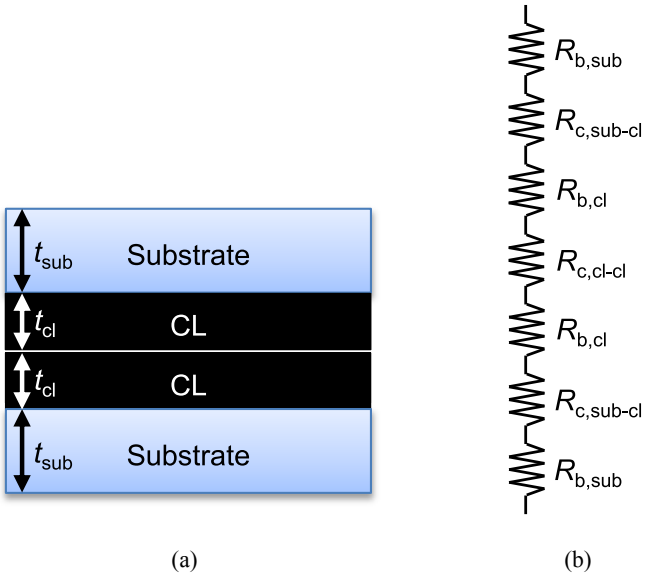

Fig. 5. Schematics of: (a) a substrate-CL-CL-substrate sandwich making one sample for the measurements, and (b) components of the through-plane bulk resistance of the sandwich.

decreasing trend of the data with increasing pressure is due to reduction in the TCRs of the test columns as pressure increases. The maximum uncertainty of $R''A$ is 2.7% for the data from the modified TPS method and 17.3% for the data from the GHF method. Reasons for having higher $R''A$ values from the modified TPS method than $R''A$ values from the GHF method are, again, the much higher bulk resistance of the ETFE substrates than the Al substrates and the existence of the Kapton layer of the TPS sensor in the TPS test column. In addition, as is also mentioned in Ref. [19], compared to the micro-patterned surfaces of the TPS sensor, flatter and pattern-free metallic surfaces of the GHF fluxmeters result in lower contact insulances in the GHF test column.

The measured values of through-plane thermal conductivity of the CLs for different pressures are plotted next to the analytical predictions of Ref. [28] in Fig. 8. The following can be concluded from Fig. 8:

1. Hot-pressing has no effect on the through-plane thermal conductivity of the CL, which is expected considering that no meaningful change was observed in the thickness of the CLs before and after hot-pressing.
2. Changing mechanical pressure from 1 to 14.5 bar has no effect on the measured thermal conductivity values. Again, this could be explained by the constant thickness of the CLs under compression as shown by the TUC_RUC measurements at different pressures for hot-pressed and non-hot-pressed catalyst-coated substrates and from the SEM measurements before and after decal-transfer. It is evident that CLs are highly incompressible.
3. The measurement method has no effect on the measured thermal conductivity values, i.e. the TPS and GHF results are consistent.
4. As expected, the type of (non-porous) substrate, studied in this work, has no effect on the through-plane thermal conductivity of the CL.
5. The analytical results of Ref. [28] predict a slight increase in the thermal conductivity of the CL with increasing pressure, up to 14% at 15 bar, which is a result of increase in the area size of point contacts between the carbon particles [28]. The model of Ref. [28] also predicts very slight compressibility of each carbon particle, which justifies the observed small increase in the analytical values of thermal conductivity and is also consistent with the thickness measurements by the TUC_RUC device at different pressures. However, as shown in Fig. 8, the slight increase in the analytical values of thermal conductivity with increasing pressure falls in the uncertainty range of the experimental data and, therefore, cannot be captured experimentally.

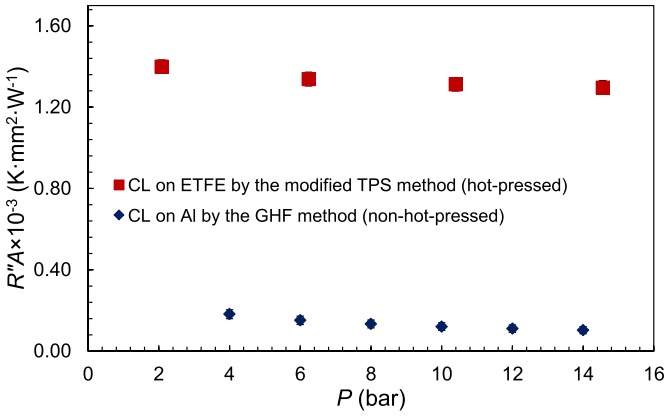

Fig. 7. $R''A$ versus pressure for the modified TPS and GHF measurements.

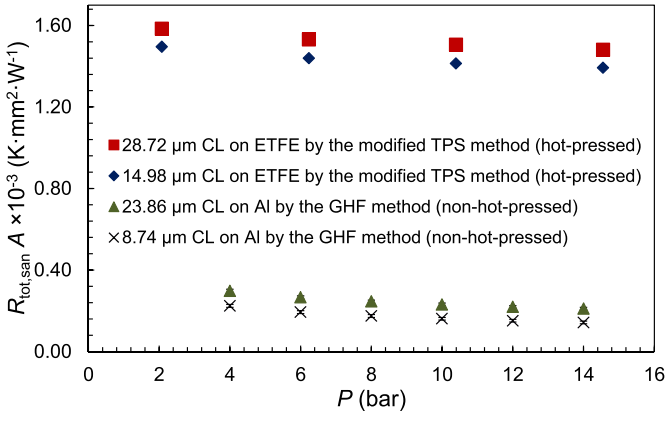

Fig. 6. Total through-plane thermal insulance versus pressure for different thicknesses of catalyst in the sandwich.

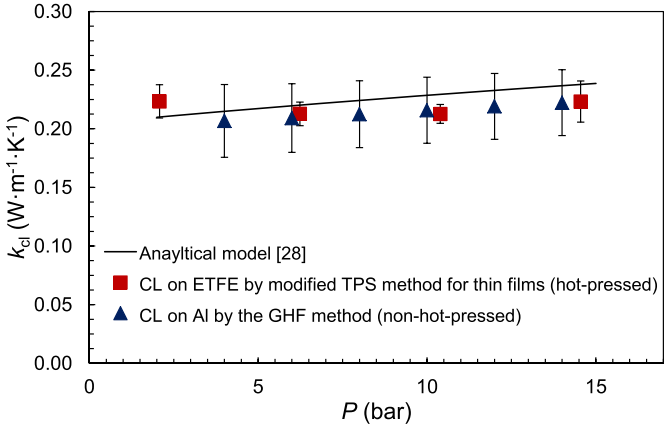

Fig. 8. Through-plane thermal conductivity of the CL versus pressure.

Table 1
Summary of the average through-plane thermal conductivity values.

Substrate	Hot-pressed?	Measurement method	k_{cl} ($W \cdot m^{-1} \cdot K^{-1}$)	Relative difference
ETFE	Yes	Modified TPS	0.218 ± 0.005	1.9%
Al	No	GHF	0.214 ± 0.005	

6. The maximum uncertainties (the confidence intervals) of the measured values of thermal conductivity, shown in Fig. 8, are 7.9% for hot-pressed CL on ETFE measured by the modified TPS method and 15.0% for non-hot-pressed CL on Al foil measured by the GHF method. The average value of through-plane thermal conductivity of the CL (along with the standard deviation from average) is 0.218 ± 0.005 $W \cdot m^{-1} \cdot K^{-1}$ from the data of hot-pressed CL on ETFE measured by the modified TPS method and 0.214 ± 0.005 $W \cdot m^{-1} \cdot K^{-1}$ from the data of non-hot-pressed CL on Al foil measured by the GHF method.

4. Conclusions

In this study, a new and rigorous procedure was developed for measuring the through-plane thermal conductivity of a CL coated on a substrate. The proposed procedure was then used to study the effects of hot-pressing, compression, measurement method, and substrate on the through-plane thermal conductivity of the CL. The tested CLs were coated by a Mayer bar on ETFE and Al substrates, and their thicknesses were measured by SEM on freeze-fractured samples to enhance the accuracy of the thermal conductivity measurements. Results showed that the through-plane thermal conductivity of the CL is not affected by any of the studied factors mentioned above. The average thermal conductivity values together with the relevant standard deviations from the averages are summarized in Table 1. It is worthy to mention here that since the authors didn't detect any statistically meaningful change in the measured thermal conductivity values with change in pressure and their analytical model also backed this experimental observation, all the measured thermal conductivity values at different pressures for each case of Table 1 could actually be regarded as repetitions of the same experiment for that case (leaving the ineffective factor of compression out), and therefore, the average of all those data points at different pressures together with the standard deviation of the data points from that average could be reported as the value of through-plane thermal conductivity of the CL for each case, as reported in Table 1.

Acknowledgements

The authors gratefully acknowledge the financial support received from the Natural Sciences and Engineering Research Council of Canada (NSERC) through NSERC Collaborative Research Development Grant no. 31-614105, Ms. Dorina Manolescu from Automotive Fuel Cell Cooperation Corp. (AFCC) for assisting in coating the CL samples by the Mayer bar, and Adrian Wikarna from Simon Fraser University (SFU) who assisted in conducting some of the thermal conductivity measurements by the TPS device during his undergraduate coop program at Laboratory for Alternative Energy Conversion (LAEC) at SFU.

References

[1] J. Wu, X.Z. Yuan, J.J. Martin, H. Wang, J. Zhang, J. Shen, S. Wu, W. Merida, A review of PEM fuel cell durability: degradation mechanisms and mitigation strategies, J. Power Sources 184 (2008) 104–119.
[2] S.G. Kandlikar, Z. Lu, Thermal management issues in a PEMFC stack-a brief review of current status, Appl. Therm. Eng. 29 (2009) 1276–1280.
[3] M. Khandelwal, M.M. Mench, Direct measurement of through-plane thermal conductivity and contact resistance in fuel cell materials, J. Power Sources 161 (2006) 1106–1115.
[4] E. Sadeghi, M. Bahrami, N. Djilali, Analytic determination of the effective thermal conductivity of PEM fuel cell gas diffusion layers, J. Power Sources 179 (2008) 200–208.
[5] J. Ramousse, S. Didierjean, O. Lottin, D. Maillet, Estimation of the effective thermal conductivity of carbon felts used as PEMFC gas diffusion layers, Int. J. Therm. Sci. 47 (2008) 1–6.
[6] E. Sadeghi, N. Djilali, M. Bahrami, Effective thermal conductivity and thermal contact resistance of gas diffusion layers in proton exchange membrane fuel cells. Part 2: hysteresis effect under cyclic compressive load, J. Power Sources 195 (2010) 8104–8109.
[7] O. Burheim, P.J.S. Vie, J.G. Pharoah, S. Kjelstrup, Ex situ measurements of through-plane thermal conductivities in a polymer electrolyte fuel cell, J. Power Sources 195 (2010) 249–256.
[8] G. Karimi, X. Li, P. Teertstra, Measurement of through-plane effective thermal conductivity and contact resistance in PEM fuel cell diffusion media, Electrochim. Acta 55 (2010) 1619–1625.
[9] E. Sadeghi, N. Djilali, M. Bahrami, Effective thermal conductivity and thermal contact resistance of gas diffusion layers in proton exchange membrane fuel cells. Part 1: effect of compressive load, J. Power Sources 196 (2011) 246–254.
[10] E. Sadeghi, N. Djilali, M. Bahrami, A novel approach to determine the in-plane thermal conductivity of gas diffusion layers in proton exchange membrane fuel cells, J. Power Sources 196 (2011) 3565–3571.
[11] N. Zamel, E. Litovsky, S. Shakhshir, X. Li, J. Kleiman, Measurement of in-plane thermal conductivity of carbon paper diffusion media in the temperature range of -20 °C to +120 °C, Appl. Energy 88 (2011) 3042–3050.
[12] O.S. Burheim, J.G. Pharoah, H. Lampert, P.J.S. Vie, S. Kjelstrup, Through-plane thermal conductivity of PEMFC porous transport layers, J. Fuel Cell Sci. Technol. 8 (2011), 021013–1-11.
[13] H. Sadeghifar, M. Bahrami, N. Djilali, A statistically-based thermal conductivity model for fuel cell gas diffusion layers, J. Power Sources 233 (2013) 369–379.
[14] N. Zamel, X. Li, Effective transport properties for polymer electrolyte membrane fuel cells – with a focus on the gas diffusion layer, Prog. Energy Combust. 39 (2013) 111–146.
[15] O.S. Burheim, G. Ellila, J.D. Fairweather, A. Labouriau, S. Kjelstrup, J.G. Pharoah, Ageing and thermal conductivity of porous transport layers used for PEM fuel cells, J. Power Sources 221 (2013) 356–365.
[16] N. Alhazmi, M.S. Ismail, D.B. Ingham, K.J. Hughes, L. Ma, M. Pourkashanian, The in-plane thermal conductivity and the contact resistance of the components of the membrane electrode assembly in proton exchange membrane fuel cells, J. Power Sources 241 (2013) 136–145.
[17] N. Alhazmi, D.B. Ingham, M.S. Ismail, K. Hughes, L. Ma, M. Pourkashanian, The through-plane thermal conductivity and the contact resistance of the components of the membrane electrode assembly and gas diffusion layer in proton exchange membrane fuel cells, J. Power Sources 270 (2014) 59–67.
[18] H. Sadeghifar, N. Djilali, M. Bahrami, Effect of Polytetrafluoroethylene (PTFE) and micro porous layer (MPL) on thermal conductivity of fuel cell gas diffusion layers: modeling and experiments, J. Power Sources 248 (2014) 632–641.
[19] M. Ahadi, M. Andisheh-Tadbir, M. Tam, M. Bahrami, An improved transient plane source method for measuring thermal conductivity of thin films: deconvoluting thermal contact resistance, Int. J. Heat. Mass Trans. 96 (2016) 371–380.
[20] N. Zamel, J. Becker, A. Wiegmann, Estimating the thermal conductivity and diffusion coefficient of the microporous layer of polymer electrolyte membrane fuel cells, J. Power Sources 207 (2012) 70–80.
[21] G. Unsworth, N. Zamel, X. Li, Through-plane thermal conductivity of the microporous layer in a polymer electrolyte membrane fuel cell, Int. J. Hydrogen Energy 37 (2012) 5161–5169.
[22] O.S. Burheim, H. Su, S. Pasupathi, J.G. Pharoah, B.G. Pollet, Thermal conductivity and temperature profiles of the micro porous layers used for the polymer electrolyte membrane fuel cell, Int. J. Hydrogen Energy 38 (2013) 8437–8447.
[23] A. Thomas, G. Maranzana, S. Didierjean, J. Dillet, O. Lottin, Thermal and water transfer in PEMFCs: investigating the role of the microporous layer, Int. J. Hydrogen Energy 39 (2014) 2649–2658.
[24] M. Andisheh-Tadbir, E. Kjeang, M. Bahrami, Thermal conductivity of microporous layers: analytical modeling and experimental validation, J. Power Sources 296 (2015) 344–351.
[25] O.S. Burheim, H. Su, H.H. Hauge, S. Pasupathi, B.G. Pollet, Study of thermal conductivity of PEM fuel cell catalyst layers, Int. J. Hydrogen Energy 39 (2014) 9397–9408.
[26] ASTM E1530-11, Standard Test Method for Evaluating the Resistance to Thermal Transmission of Materials by the Guarded Heat Flow Meter Technique, ASTM International, West Conshohocken, PA, 2011. www.astm.org.
[27] B.M. Zawilski, R.T. Littleton IV, T.M. Tritt, Description of the parallel thermal conductance technique for the measurement of the thermal conductivity of small diameter samples, Rev. Sci. Instrum. 72 (2001) 1770–1774.

[28] M. Ahadi, A. Putz, J. Stumper, M. Bahrami, Thermal conductivity of catalyst layer of polymer electrolyte membrane fuel cells: Part 2 – analytical modeling, J. Power Sources 354 (2017) 215–228.

[29] O.S. Burheim, M.A. Onsrud, J.G. Pharoah, F. Vullum-Bruer, P.J.S. Vie, Thermal conductivity, heat sources and temperature profiles of li-ion batteries, ECS Trans. 58 (2014) 145–171.